Alkyl dehydrogenation in a Rh(I) complex *via* an isolated agostic intermediate†

Adrian B. Chaplin,[a] Amalia I. Poblador-Bahamonde,[b] Hazel A. Sparkes,[c] Judith A. K. Howard,*[c] Stuart A. Macgregor*[b] and Andrew S. Weller*[a]

Received (in Cambridge, UK) 24th September 2008, Accepted 31st October 2008
First published as an Advance Article on the web 19th November 2008
DOI: 10.1039/b816739g

A well-characterised 14-electron rhodium phosphine complex, $[Rh(P^iPr_3)_3][BAr^F_4]$, which contains a β-CH agostic interaction, is observed to undergo spontaneous dehydrogenation to afford $[Rh(P^iPr_3)_2(P^iPr_2(C_3H_5))][BAr^F_4]$; calculations on a model system show that while C–H activation is equally accessible from the β-CH agostic species or an alternative γ-CH agostic isomer, subsequent β-H-transfer can only be achieved along pathways originating from the β-CH agostic form.

Transition metal-mediated alkane dehydrogenation is an important methodology for the selective transformation of alkanes.[1] The putative intermediates for such reactions are alkane sigma complexes, which then undergo successive C–H activation and β-H-elimination. For the intramolecular dehydrogenation of alkyl groups it is accepted that C–H activation is usually preceded by a M···HC agostic interaction (Scheme 1);[2] however, well-defined examples of such complexes that subsequently undergo alkyl dehydrogenation are, to the best of our knowledge, unknown. Indeed, as far as we are aware, there is only one example of a complex where an agostic interaction undergoes C–H activation for which both the agostic and C–H activated product have been crystallographically characterised,[3] and only a few examples where these tautomers are directly observed in solution.[4]

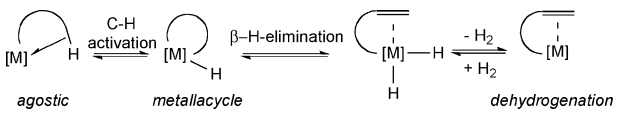

Scheme 1

We report here the isolation of a "T-shaped" 14-electron rhodium phosphine complex, $[Rh(P^iPr_3)_3][BAr^F_4]$ [**1**, Ar^F = 3,5-$C_6H_4(CF_3)_2$], that contains an unusual β-CH agostic interaction from the isopropyl phosphine ligand and undergoes intramolecular dehydrogenation. We also demonstrate, using computational methods, that the β-agostic interaction in **1** is important in defining the ultimate product of the reaction: dehydrogenation (C–H activation/β-elimination[5–7]) *versus* metallacyclobutane formation (C–H activation only[8,9]) which arises from an alternative γ-agostic interaction.

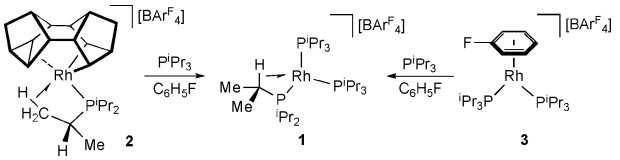

Scheme 2

Reaction of $[Rh(BINOR\text{-}S)(P^iPr_3)][BAr^F_4]$ (**2**)[10] with 2 equivalents of P^iPr_3 in C_6H_5F solution results in reductive elimination of BINOR-S and the formation of **1** in quantitative yield by NMR spectroscopy. Alternatively, **1** can be formed by the addition of P^iPr_3 to $[Rh(C_6H_5F)(P^iPr_3)_2][BAr^F_4]$ (**3**) in C_6H_5F (Scheme 2). Complex **1** is highly fluxional in solution at room temperature, displaying one phosphine environment by ^{31}P NMR spectroscopy which shows coupling to ^{103}Rh (δ 47.1, d, J_{RhP} = 173 Hz). This fluxional behaviour is not frozen out, even upon cooling to 200 K, where the $^{31}P\{^1H\}$ NMR spectrum shows a very broad signal. The ^1H NMR spectrum shows a featureless hydride region at all temperatures. In the solid state‡ (Fig. 1) the structure displays a distorted square planar geometry in which a β-CH agostic interaction from an isopropyl group occupies the fourth coordination site, showing a relatively short Rh1–C1a distance [2.494(12) Å, located Rh1–H1a 1.91(9) Å][11] and an acute Rh1–P1–C1a angle

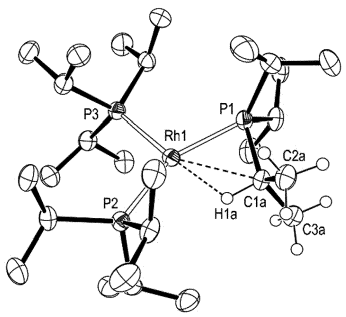

Fig. 1 Complex **1**; ellipsoids are depicted at the 50% probability level. The anion, most H atoms and minor component (**4**) are omitted for clarity. Key bond lengths (Å) and angles (°): Rh1–P1, 2.249(2); Rh1–P2, 2.395(2); Rh1–P3, 2.268(2); P1–Rh1–P2, 149.91(6); P1–Rh1–P3, 104.24(6); P2–Rh1–P3, 105.47(6); Rh1–C1a, 2.494(12); Rh1–H1a, 1.91(9); Rh1–P1–C1a, 73.8(4); C1a–C2a, 1.540(13); C1a–C3a, 1.540(13).

[a] *Department of Inorganic Chemistry, University of Oxford, UK OX1 3QR. E-mail: andrew.weller@chem.ox.ac.uk*
[b] *School of EPS – Chemistry, Heriot-Watt University, Edinburgh, UK EH14 4AS. E-mail: S.A.Macgregor@hw.ac.uk*
[c] *Department of Chemistry, University Science Laboratories, South Road, Durham, UK DH1 3LE. E-mail: j.a.k.howard@durham.ac.uk*

† Electronic supplementary information (ESI) available: Full experimental, characterisation and crystallographic details. Energies and Cartesian coordinates of all computed species; full reference for Gaussian 03. See DOI: 10.1039/b816739g/

[73.8(4)°]. The RhP_3 core is planar [sum of angles 359.6(1)°]. Complex **1** is a rare example of a formally 14-electron late-transition metal complex,[9–13] and is closely related to $[Rh(PPh_3)_3][ClO_4]$[13] and $Rh(^tBu_2PCH_2P^tBu_2)(CH_2Me_3)$.[12a]

Isopropyl phosphine groups have been shown to coordinate through γ-agostic interactions,[9,10,14] but as far as we are aware **1** is the first structurally characterised example of a β-agostic interaction with this ligand motif. Given the fluxional behaviour of **1**, even at 200 K, we have not been able to determine experimentally whether this interaction dominates in solution, or rapidly interconverting β- or γ-interactions are present. We did not observe a clear C–H stretch in the IR spectrum that could be assigned to the agostic C–H bond.

Complex **1** spontaneously,[6,16] but slowly ($t_{1/2}$ ~ 1.5 h), undergoes dehydrogenation of one of the isopropyl substituents in solution at room temperature (C_6H_5F solvent). This results in the generation of an equilibrium mixture of $[Rh(P^iPr_3)_2(\eta^3\text{-}P^iPr_2(C_3H_5))][BAr^F_4]$ (**4**) and $[RhH_2(P^iPr_3)_3][BAr^F_4]$ (**5**)—see ESI† for full details including a solid-state structure—the latter of which arises from reaction of **1** with liberated H_2 (**1**:**4**:**5** = 1.0:0.95:0.35) (Scheme 3). **5** is closely related to previously reported $[IrH_2(P^iPr_2Ph)_3][BAr^F_4]$.[15] Due to this process and the structural similarity of **4**, isolation of **1** by crystallisation at low temperature occurs concomitant with small amounts of **4** (**1**:**4** ~ 4:1 on the basis of integrals in the ^1H NMR spectrum and X-ray diffraction). The dehydrogenation/hydrogenation equilibrium in solution is shifted towards **4** by successive removal of hydrogen through freeze–vacuum–thaw cycles, while addition of the hydrogen acceptor *t*-butylethene (*t*be) results in the clean formation of **4** (86% isolated yield). Addition of H_2 to **1** or **4** rapidly generates **5**, the latter presumably *via* **1**, showing that the dehydrogenation is reversible. In CH_2Cl_2 or THF dehydrogenation of **1** also occurs alongside decomposition to unidentified products.

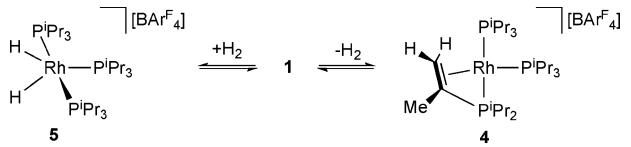

Scheme 3

The solid-state‡ structure of isolated **4** is shown in Fig. 2 and confirms dehydrogenation of one of the isopropyl groups to form an η^3-coordinated vinyl phosphine. The rhodium has an approximately square planar geometry, and the featureless high-field region of the ^1H NMR spectrum of **4** (200 K) supports the lack of a hydride ligand. The molecular geometry and structural metrics of the η^3-ligand are similar to those reported previously for vinyl phosphines.[6,7]

Mechanistically, phosphine dissociation during the dehydrogenation reaction is discounted as no inhibition is observed in the presence of excess phosphine (10 equivalents), while no dehydrogenation is observed for **3** in C_6H_5F. These observations suggest successive C–H activation and β-elimination in **1** followed by loss of dihydrogen (Scheme 1). Two questions thus arise: does C–H activation occur at the β or γ position, and how does this affect the ultimate outcome of the reaction (dehydrogenation *versus* cyclometallation)?

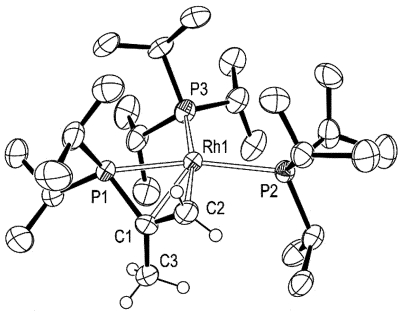

Fig. 2 Complex **4**; ellipsoids are depicted at the 50% probability level, the anion and most H atoms have been omitted for clarity. Key bond lengths (Å) and angles (°): Rh1–P1, 2.291(2); Rh1–P2, 2.395(2); Rh1–P3, 2.347(2); P1–Rh1–P2, 153.93(6); P1–Rh1–P3, 99.10(6); P2–Rh1–P3, 106.63(5); Rh1–C1, 2.183(6); Rh1–C2, 2.240(6); Rh1–P1–C1, 63.6(2); C1–C2, 1.399(8); C1–C3, 1.489(8).

To address these issues we have employed density functional theory calculations[17] to study the reactivity of the model cation, $[Rh(PH_2{}^iPr)(PH_3)_2]^+$, **1′**. Three forms of **1′** were located, **1′β** and **1′γ**, with β- and γ-CH agostic interactions, respectively (Fig. 3), as well as an anagostic form, **1′an**. For the simple model system **1′γ** is more stable than **1′β**, reflecting the lesser degree of strain associated with the five-membered Rh–P–C–C–H ring in this case. Although this is contrary to what is observed in the solid-state structure our model does not take into account the effects of ligand bulk which can play a significant role in determining the nature of an agostic interaction.[15] In addition solid-state packing effects may play a role in favouring one agostic form over the other. **1′β** and **1′γ** are linked *via* **1′an** (E = 2.9 kcal mol^{-1}), the highest point along this pathway being loss of the β-CH agostic *via* a TS at 5.9 kcal mol^{-1}. **1′an** corresponds to a very shallow minimum and forms **1′γ** with a negligible barrier (not shown in Fig. 3). The low overall activation energies for interconversion between **1′β** and **1′γ** are consistent with the highly fluxional behaviour observed in the NMR spectra of **1**.

C–H activation TS structures were located from both **1′β** and **1′γ** and the computed activation barriers of 11.9 kcal mol^{-1} and 11.5 kcal mol^{-1}, respectively, indicate that these processes are equally accessible. C–H activation is also endothermic and should be reversible. Importantly, the accessibility of the initial C–H activation does not depend significantly on the nature of the CH agostic bond present in the reactant.

In contrast, β-H-transfer in the C–H activated species **6′β** and **6′γ** depends markedly on which intermediate is involved.

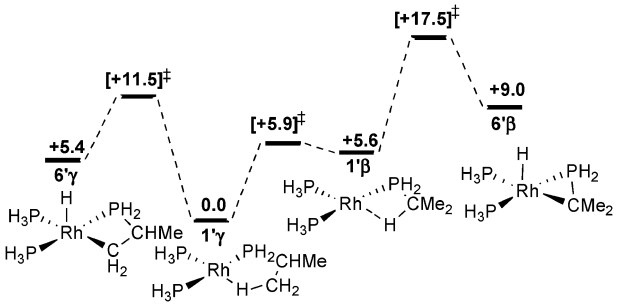

Fig. 3 Reaction profiles (kcal mol^{-1}) for C–H activation in **1′β** and **1′γ**.

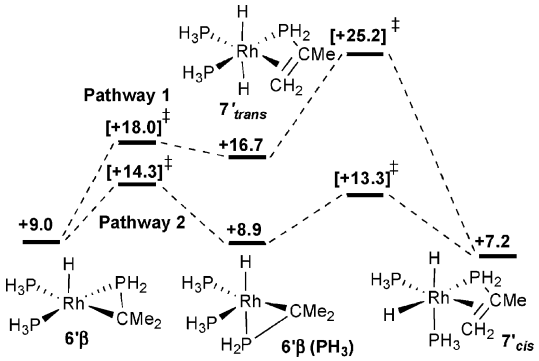

Fig. 4 Reaction profiles (kcal mol^{-1}) for β-H-transfer in **6′β**.

For metallacyclophosphabutane **6′γ**, we were unable to locate a TS for β-H-transfer to Rh. Scans based on the Rh-βH distance led to a steady increase in energy to over 30 kcal mol^{-1} above **6′γ**. TS structures were located but these were shown to be for a Rh-assisted 1,2 H shift resulting in isomerisation to **6′β** (E = +31.1 kcal mol^{-1}, see ESI†). For **6′β**, however, a number of low energy β-H-transfer pathways were characterised, two of which are shown in Fig. 4. In order to complete the dehydrogenation process a *cis*-dihydride must be formed upon β-H-transfer so that H_2 reductive elimination can be accessed. In Pathway 1 this is achieved by initial β-H-transfer from **6′β** to form *trans*-dihydride **7′$_{trans}$**, (E = +16.7 kcal mol^{-1}) followed by isomerisation to **7′$_{cis}$**. The *cis–trans* isomerisation TS is the highest point along Pathway 1 (E = +25.2 kcal mol^{-1}) and corresponds to a barrier of 19.6 kcal mol^{-1} relative to **1′β**. Alternatively, isomerisation of square-pyramidal **6′β** (where H is apical) occurs prior to β-H-transfer. The lowest energy mechanism of this type, Pathway 2, proceeds *via* a PH_3 apical isomer (**6′β(PH$_3$)**, E = +8.9 kcal mol^{-1}) from which β-H-transfer leads to **7′$_{cis}$**. The isomerisation TS is the highest point along Pathway 2 (E = +14.3 kcal mol^{-1}) equating to a barrier of only 8.7 kcal mol^{-1} relative to **1′β**. A second isomerisation/β-H-transfer route *via* isomer **6′β(PH$_3$)** (with {PH_2} apical) was also defined, Pathway 3. This was energetically intermediate with regard to Pathways 1 and 2 with an overall barrier of 13.4 kcal mol^{-1}, the highest TS being for β-H-transfer at +19.0 kcal mol^{-1}. Full details are given in the ESI†.

To complete the dehydrogenation, reductive elimination of H_2 from **7′$_{cis}$** is required and a TS for this process was located at +15.1 kcal mol^{-1}. For Pathway 2 this is the highest point in the overall process, although for Pathways 1 and 3 this occurs earlier in the profile (either *cis–trans* isomerisation or β-H-transfer, respectively). The model products, **4′** + H_2, have a computed relative energy of +9.0 kcal mol^{-1}, although the entropy associated with H_2 dissociation means that the free energy of the products is only +2.9 kcal mol^{-1} above **1′β**, consistent with the reversibility of the dehydrogenation.

In conclusion we report a "14-electron" T-shaped Rh(I) complex with a supporting β-agostic interaction from an isopropyl phosphine that spontaneously undergoes dehydrogenation (C–H activation followed by β-H-transfer). Calculations show that while both γ- and β-agostic interactions can undergo reversible C–H activation to give metallacycle intermediates, subsequent H-transfer is only accessible when originating from the β-agostic form. Therefore only the product of C–H activation at the β-position can lead to productive dehydrogenation.

Notes and references

‡ *Crystallographic data*. **1**: $C_{59}H_{74.6}BF_{24}P_3Rh$, M = 1446.42, monoclinic, $P2_1/n$ (Z = 4), a = 13.1039(6) Å, b = 28.652(1) Å, c = 17.9634(8) Å, β = 106.228(1)°. V = 6475.6(5) Å^3, T = 120(2) K, 13 255 unique reflections [R(int) = 0.0395]. Final R_1 = 0.0455 [$I > 2\sigma(I)$]. **4**: $C_{59}H_{73}BF_{24}P_3Rh$, M = 1444.80, monoclinic, $P2_1$ (Z = 6), a = 19.3219(2) Å, b = 17.7292(2) Å, c = 29.0445(3) Å, β = 96.6182(4)°. V = 9883.2(2) Å^3, T = 150(2) K, 31 319 unique reflections [R(int) = 0.0396]. Final R_1 = 0.0506 [$I > 2\sigma(I)$].

1 (*a*) C. M. Jensen, *Chem. Commun*., 1999, 2443; (*b*) R. H. Crabtree, *J. Chem. Soc., Dalton Trans*., 2001, 2437; (*c*) A. S. Goldman, A. H. Roy, Z. Huang, R. Ahuja, W. Schinski and M. Brookhart, *Science*, 2006, **312**, 257.

2 (*a*) G. J. Kubas, *Metal Dihydrogen and σ-Bond Complexes*, Kluwer Academic/Plenum Publishers, New York, 2001; (*b*) M. Brookhart, M. L. H. Green and G. Parkin, *Proc. Natl. Acad. Sci. U. S. A*., 2007, **104**, 6908.

3 N. M. Scott, R. Dorta, E. D. Stevens, A. Correa, L. Cavallo and S. P. Nolan, *J. Am. Chem. Soc*., 2005, **127**, 3516.

4 (*a*) A. C. Albeniz, G. Schulte and R. H. Crabtree, *Organometallics*, 1992, **11**, 242; (*b*) B. Rybtchinski, L. Konstantinovsky, L. J. W. Shimon, A. Vigalok and D. Milstein, *Chem.–Eur. J*., 2000, **6**, 3287; (*c*) D. Buccella and G. Parkin, *J. Am. Chem. Soc*., 2006, **128**, 16358; (*d*) A. Toner, J. Matthes, S. Gruendemann, H. Limbach, B. Chaudret, E. Clot and S. Sabo-Etienne, *Proc. Natl. Acad. Sci. U. S. A*., 2007, **104**, 6945; (*e*) L. Mole, J. L. Spencer, N. Carr and A. G. Orpen, *Organometallics*, 1991, **10**, 49.

5 M. Baya, M. L. Buil, M. A. Esteruelas and E. Onate, *Organometallics*, 2004, **23**, 1416–1423.

6 P. B. Glaser and T. D. Tilley, *Organometallics*, 2004, **23**, 5799.

7 A. J. Edwards, M. A. Esteruelas, F. J. Lahoz, A. M. Lopez, E. Onate, L. A. Oro and J. I. Tolosa, *Organometallics*, 1997, **16**, 1316.

8 (*a*) D. L. Thorn, *Organometallics*, 1998, **17**, 348; (*b*) N. Thirupathi, D. Amoroso, A. Bell and J. D. Protasiewicz, *Organometallics*, 2005, **24**, 4099.

9 M. J. Ingleson, M. F. Mahon and A. S. Weller, *Chem. Commun*., 2004, 2398.

10 S. Brayshaw, J. Green, G. Kociok-Köhn, E. Sceats and A. S. Weller, *Angew. Chem., Int. Ed*., 2006, **45**, 452.

11 W. Baratta, C. Mealli, E. Herdtweck, A. Ienco, S. A. Mason and P. Rigo, *J. Am. Chem. Soc*., 2004, **126**, 5549.

12 (*a*) H. Urtel, C. Meier, F. Eisentrager, F. Rominger, J. P. Joschek and P. Hofmann, *Angew. Chem., Int. Ed*., 2001, **40**, 781; (*b*) P. H. M. Budzelaar, N. N. P. Moonen, R. de Gelder, J. M. M. Smits and A. W. Gal, *Eur. J. Inorg. Chem*., 2000, 753; (*c*) W. Baratta, S. Stoccoro, A. Doppiu, E. Herdtweck, A. Zucca and P. Rigo, *Angew. Chem., Int. Ed*., 2003, **42**, 105; (*d*) A. Y. Verat, M. Pink, H. Fan, J. Tomaszewski and K. G. Caulton, *Organometallics*, 2008, **27**, 166, and references therein.

13 Y. W. Yared, S. L. Miles, R. Bau and C. A. Reed, *J. Am. Chem. Soc*., 1977, **99**, 7076.

14 H. Aneetha, M. Jimenez-Tenorio, M. C. Puerta, P. Valerga, V. N. Sapunov, R. Schmid, K. Kirchner and K. Mereiter, *Organometallics*, 2002, **21**, 5334.

15 A. C. Cooper, E. Clot, J. C. Huffman, W. E. Streib, F. Maseras, O. Eisenstein and K. G. Caulton, *J. Am. Chem. Soc*., 1999, **121**, 97–106.

16 (*a*) T. M. Douglas and A. S. Weller, *New J. Chem*., 2008, **32**, 966; (*b*) T. M. Douglas, S. K. Brayshaw, R. Dallanegra, G. Kociok-Köhn, S. A. Macgregor, G. Moxham, A. S. Weller, T. Wondimagegn and P. Vadivelu, *Chem.–Eur. J*., 2008, **14**, 1004; (*c*) T. M. Douglas, H. Le Notre, S. K. Brayshaw, C. G. Frost and A. S. Weller, *Chem. Commun*., 2006, 3408.

17 Calculations employed Gaussian 03 with the BP86 functional. Rh and P centres were described with Stuttgart RECPs and basis sets with polarisation on P. 6-31G** basis sets were used for C and H atoms. All energies include a correction for zero-point energies. See ESI† for full details.

